Electronic Supplementary Material (ESI) for Chemical Communications.
This journal is © The Royal Society of Chemistry 2016

Supporting Information

Smart adsorbents with reversible photo-regulated molecular switches for selective adsorption and efficient regeneration

Jing Zhu, Peng Tan, Piao-Ping Yang, Xiao-Qin Liu,* Yao Jiang, and Lin-Bing Sun*

Jiangsu National Synergetic Innovation Center for Advanced Materials (SICAM), State Key Laboratory of Materials-Oriented Chemical Engineering, College of Chemistry and Chemical Engineering, Nanjing Tech University, Nanjing 210009, China.

E-mail: liuxq@njtech.edu.cn; lbsun@njtech.edu.cn

Additional Background

In recent years, bio-inspired synthetic strategies for functional materials have gained lots of attention.[1] Implementation of switchable molecules to fabricate man-made materials can endow them with some interesting properties, for example, in response to external stimuli (e.g. light, thermal, magnet, and pH).[2] Researches on photo-regulated materials have been carried out extensively because light as an external stimulus possessing unique advantages compared to other kinds of stimulus.[3] The behavior of switchable molecules can be controlled by light remotely and applied/removed instantaneously. Besides, the light can be delivered to a central position precisely. Therefore, aboundant photo-regulated materials applied in various fields have been investigated, taking light as external stimulus.[4] Here we report the fabrication of smart adsorbents by introducing an azobenzene derivative 4-(3-triethoxysilylpropyl-ureido) azobenzene (AB-TPI) to pore interiors of mesoporous silica MCM-41.

Experimental Section

Materials Synthesis.

Synthesis of 4-(3-triethoxysilylpropyl-ureido) azobenzene (AB-TPI). The compound AB-TPI was obtained as follows.[5] Under dry N_2, 2.05 g of triethoxysilylpropyl isocyanate (TESPIC) (8.12 mmol) and 1.58 g of 4-phenylazoaniline (PAA) (7.85 mmol) were added in 12 mL of anhydrous tetrahydrofuran (THF). The resulting mixture was then boiled under reflux for 12 h. After refluxing, 40 mL of *n*-hexane was added to facilitate the crystalization of AB-TPI at a low temperature (–20 °C). The resulting shiny needle-like orange crystals recrystallized from the hexane solution after 12 h and the compound was dried in vacuo.

Preparation of Azobenzene-Modified Mesoporous Silica (AM) Samples. The AM samples were synthesized as follows. The co-condensation method (one-pot synthesis) was adopted to prepare azobenzene-modified mesostructured silica.[6] Typically synthesis, 3.5 mL of NaOH (2 M) solution was mixed with 240 mL of distilled water. The solution was heating to 80 ^{o}C with stirring after 1.0 g of template cetyltrimethylammonium bromide (CTAB) was added. When the solution became homogeneous, 5 mL of tetraethyl orthosilicate (TEOS) was added

dropwise, giving rise to a white slurry. Then the ethanol solution (5 mL) of certain weight of AB-TPI was added dropwise at once. The amounts of AB-TPI compound used in synthesis procedure were 0.0715, 0.1430, 0.2220, and 0.2860 g respectively. After 2 h, the resulting product was filtered, washed with distilled water, and dried at 80 ^{o}C for 12 h, which leads to the formation of as-synthesized AM samples.

Then the obtained samples with surfactant were refluxed in 100 mL of ethanol containing 1mL of HCl (1 M) at 80 °C for 4 h. This process was carried out twice to ensure the complete removal of surfactant from the pores of adsorbents. The obtained solid was filtered off, washed with ethanol and water, and finally dried at 80 °C for 12 h. The materials modified with different amounts of AB-TPI were denoted as AM-1, AM-2, AM-3, and AM-4, corresponding to the data of TG and elemental analyses.

Characterization.

X-ray diffraction (XRD) patterns of the materials were recorded using a Bruker D8 Advance diffractometer with monochromatic Cu Kα radiation in the 2θ range from 1^{o} to 6^{o} and 10^{o} to 80^{o} at 40 kV and 40 mA. Scanning electron microscopy (SEM) and energy dispersive X-ray spectroscopy (EDX) analyses were performed using a FEI Magellan 400 (USA) electron microscope. N_2 adsorption-desorption isotherms were measured using ASAP 2020 at –196 ^{o}C. The temperature selected to perform the degasification step was 80 ^{o}C, and the degasification time was 4 h. The Brunauer-Emmett-Teller (BET) surface area was calculated using adsorption data in a relative pressure ranging from 0.04 to 0.20. The total pore volume was determined from the amount adsorbed at a relative pressure of about 0.99. The pore size distribution of the mesoporous materials was calculated from the adsorption branch by using the Barrett–Joyner–Halenda (BJH) method. Fourier transform infrared (IR) spectra of the samples diluted with KBr were carried out on a Nicolet Nexus 470 spectrometer with a spectra resolution of 2 cm^{-1}. Thermogravimetric (TG) and differential thermogravimetric (DTG) analyses were carried out in a N_2 flow from room temperature to 800 ^{o}C on a TG209F1 apparatus. Diffuse reflectance UV-vis spectroscopy were obtained with a UV-2401PC spectrophotometer, and $BaSO_4$ was used as an internal standard. ^{1}H (nuclear magnetic resonance) (NMR, 300 MHz) were measured on a Bruker AVANCE 400

spectrometer in dimethyl sulfoxide. The dye content of the treated solutions was determined using a Lambda 35 spectrometer (Pekin-Elmer). The molecular size estimation was carried out using Materials Studio (Accelrys). The elemental analysis (C, H, N, and S) was performed by a Vario Micro Cube elemental analyzer (Elementar Analysensysteme GmbH, Hanau, Germany).

Adsorption Test.

Two dyes were used as adsorbates for selective adsorption study, neutral red (NR) and the Coomassie brilliant blue (CBB). The contents of guest molecules in aqueous solutions were both 25 $mg \cdot L^{-1}$. Adsorption experiments were performed in the quartz cuvette directly in the cell holder of UV-vis spectrophotometer under ambient conditions. In a typical adsorption experiment, 2 mg of the adsorbent was statically dispersed in the aqueous solution (3 mL) containing 25 $mg \cdot L^{-1}$ of guest molecules, until the adsorption equilibrium was reached. The contents of guest molecules in the treated solutions were determined at regular intervals using the UV-vis spectrophotometer. For comparison, another portion of samples were irradiated with UV light for 180 min (wavelength >310 nm) using a xenon lamp (CEL-HXUV300) equipped with a filter. The coolant was used to prevent the samples from heating up. After photo-irradiation, the samples were used for the same adsorption experiments as above. The dye concentration was detected using a UV-vis spectrophotometer at appropriate time intervals. The adsorption amount (Q_e) was determined according to formula (1).

$$Q_e = \frac{(c_i - c_e)V}{m} \qquad (1)$$

Where c_i is the initial concentration, c_e is the residual or equilibrium concentration, V is the volume of liquid phase, and m is the mass of adsorbent.

Desorption was carried out by using saturated adsorbents in the mixture of ethanol/water solution. The selection of desorption solvent in the desorption process of NR molecules on mesoporous silica MCM-41, which is a kind of polar adsorbents, is based on the principle of similar polarity. The polarity of ethanol is weaker than water, and NR molecules are of weak polarity. Therefore, it is favorable for the elution of NR molecules from adsorbents with ethanol/water solution. The dye concentration was measured at appropriate time intervals by

UV-vis spectrophotometer and the desorption amount (Q_d) was determined according to formula (2).

$$Q_d = \frac{c_d V}{m Q_e} \times 100\% \qquad (2)$$

Where c_d is the desorption equilibrium concentration.

References

1 (a) N. Yanai, T. Uemura, M. Inoue, R. Matsuda, T. Fukushima, M. Tsujimoto, S. Isoda and S. Kitagawa, *J. Am. Chem. Soc.*, 2012, **134**, 4501; (b) A. Coskun, M. Banaszak, R. D. Astumian, J. F. Stoddart and B. A. Grzybowski, *Chem. Soc. Rev.*, 2012, **41**, 19; (c) D. H. Qu, Q. C. Wang, Q. W. Zhang, X. Ma and H. Tian, *Chem. Rev.*, 2015, **115**, 7543; (d) K. Nomoto, S. Kume and H. Nishihara, *J. Am. Chem. Soc.*, 2009, **131**, 3830; (e) S. Mura, J. Nicolas and P. Couvreur, *Nature Mater.*, 2013, **12**, 991.

2 (a) Y. Klichko, M. Liong, E. Choi, S. Angelos, A. E. Nel, J. F. Stoddart, F. Tamanoi and J. I. Zink, *J. Am. Ceram. Soc.*, 2009, **92**, S2; (b) J. Zhang, Q. Zou and H. Tian, *Adv. Mater.*, 2013, **25**, 378; (c) T. Muraoka, K. Kinbara and T. Aida, *J. Am. Chem. Soc.*, 2006, **128**, 11600; (d) Q. Sun, Z. Li, D. J. Searles, Y. Chen, G. Q. Lu and A. J. Du, *J. Am. Chem. Soc.*, 2013, **135**, 8246.

3 P. K. Kundu, D. Samanta, R. Leizrowice, B. Margulis, H. Zhao, M. Börner, UdayabhaskararaoT, D. Manna and R. Klajn, *Nature Chem.*, 2015, **7**, 646.

4 (a) D. Bruhwiler, *Nanoscale*, 2010, **2**, 887; (b) N. Huang, X. Ding, J. Kim, H. Ihee and D. Jiang, *Angew. Chem., Int. Ed.*, 2015, **54**, 8704; (c) L. Zhao, D. A. Loy and K. J. Shea, *J. Am. Chem. Soc.*, 2006, **128**, 14250.

5 N. Liu, D. R. Dunphy, M. A. Rodriguez, S. Singer and J. Brinker, *Chem. Commun.*, 2003, **10**, 1144.

6 F. Hoffmann, M. Cornelius, J. Morell and M. Froba, *Angew. Chem., Int. Ed.*, 2006, **45**, 3216.

Table S1. Physicochemical Properties of Different Samples

Sample	Content of AB derivatives[a] (wt %)	S_{BET}[b] (m^2/g)	D_p[c] (nm)	V_p[d] (cm^3/g)	Elemental composition[e] (wt%)		
					N	C	H
MCM-41	0	1135	2.63	0.81	0	2.05	2.80
AM-1	7.5	1076	2.96	0.93	0.95	5.20	2.93
AM-2	13.6	1019	2.77	0.88	1.72	8.79	3.11
AM-3	17.3	986	2.69	0.85	2.18	9.61	3.21
AM-4	21.7	968	2.63	0.82	2.74	11.86	3.33

[a] The introduced amount was calculated according to elemental analysis. [b] The BET surface area was calculated using adsorption data in relative pressures ranging from 0.04 to 0.20. [c] The pore size distribution was calculated from the adsorption isotherm by using the BJH method. [d] The pore volume was determined from the amount adsorbed at a relative pressure of about 0.99. [e] The elemental composition was analyzed by a Vario Micro Cube elemental analyzer.

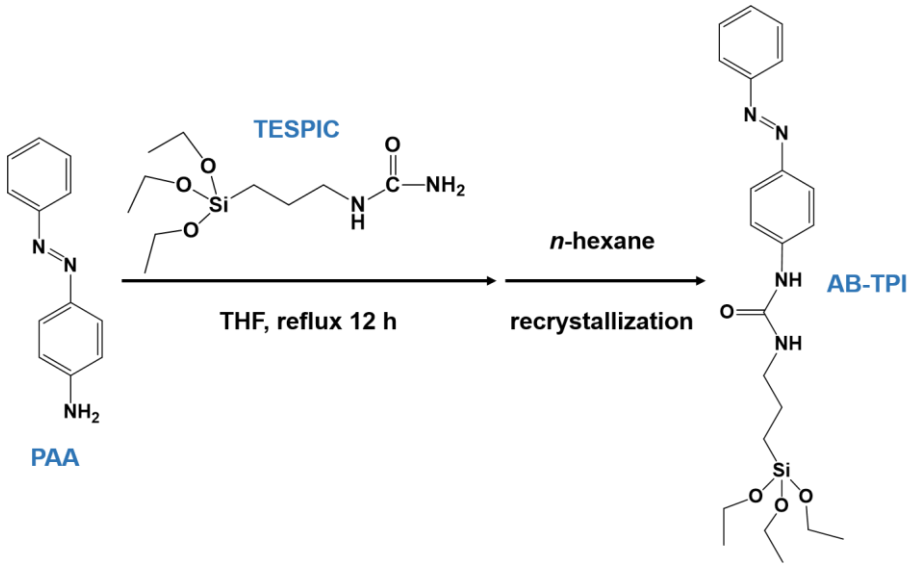

Figure S1. The synthetic process of AB-TPI.

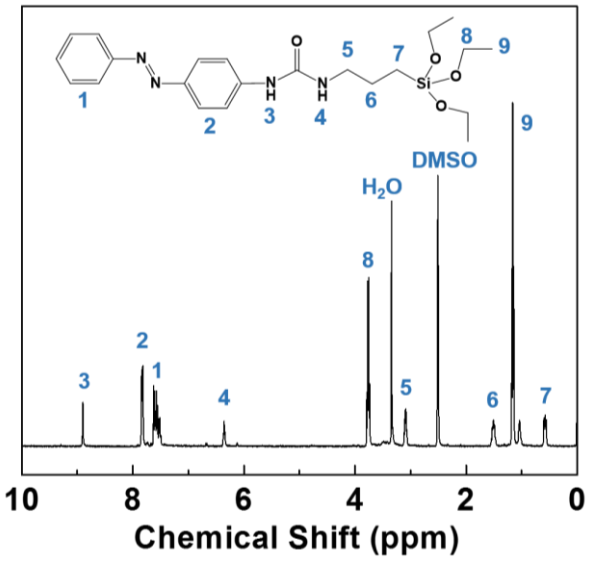

Figure S2. ^{1}H NMR spectrum of AB-TPI in dimethyl sulfoxide.

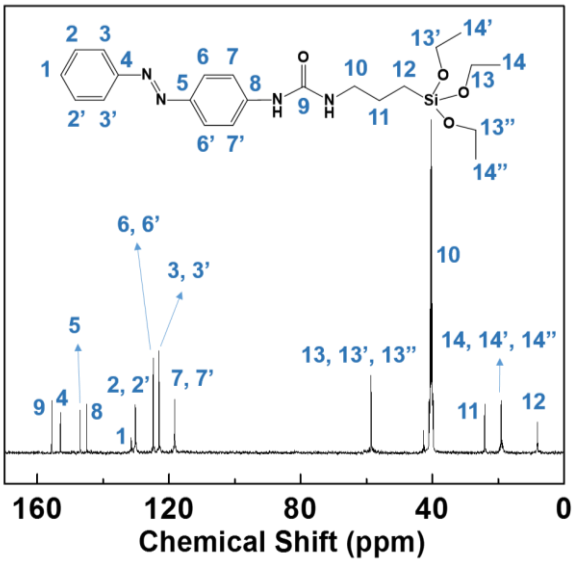

Figure S3. ^{13}C NMR spectrum of AB-TPI in dimethyl sulfoxide.

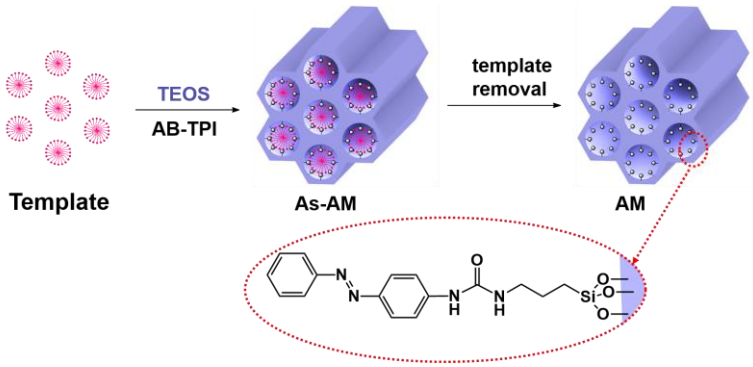

Figure S4. The synthetic process of AB-modified MCM-41.

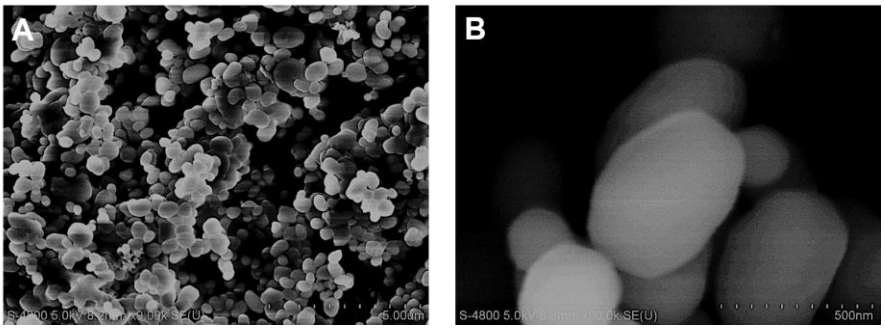

Figure S5. SEM images of the sample MCM-41.

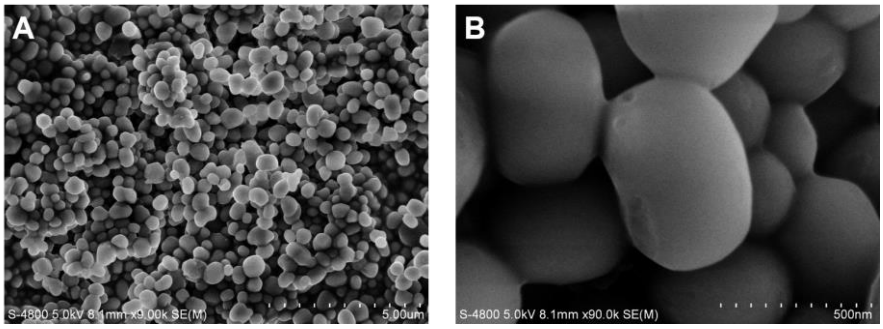

Figure S6. SEM images of the sample AM-3.

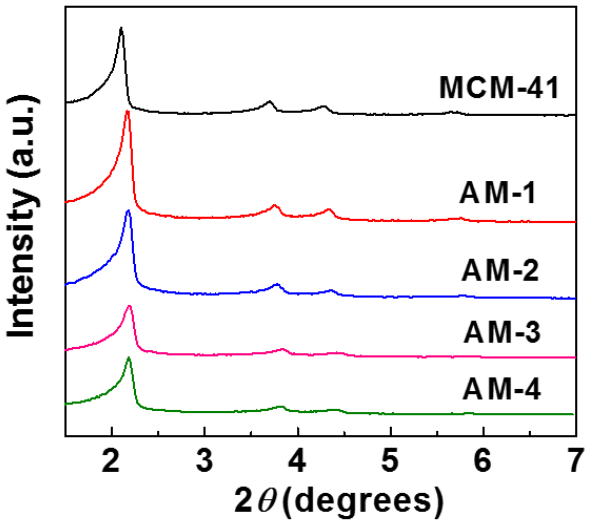

Figure S7. Low-angle XRD patterns of MCM-41 and AB-modified MCM-41 samples.

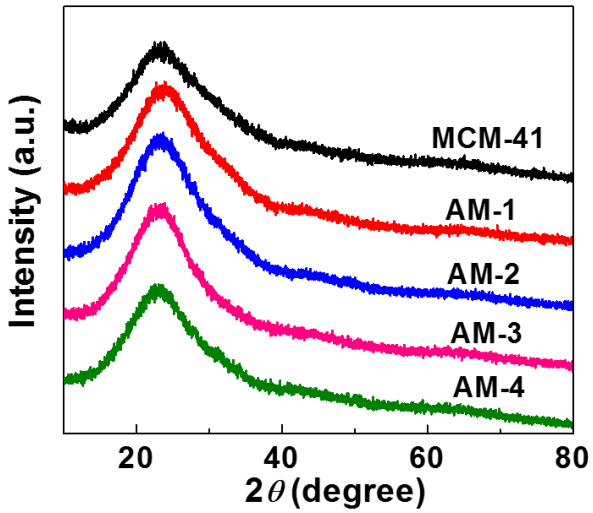

Figure S8. Wide-angle XRD patterns of MCM-41 and AB-modified MCM-41 samples.

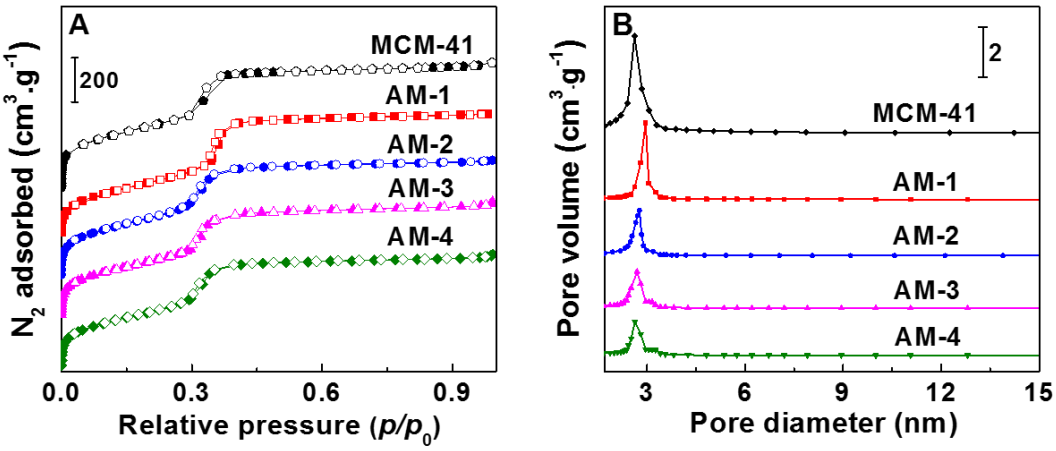

Figure S9. (A) N_2 adsorption-desorption isotherms and (B) pore size distributions of the sample AM-3. Curves are plotted offset for clarity.

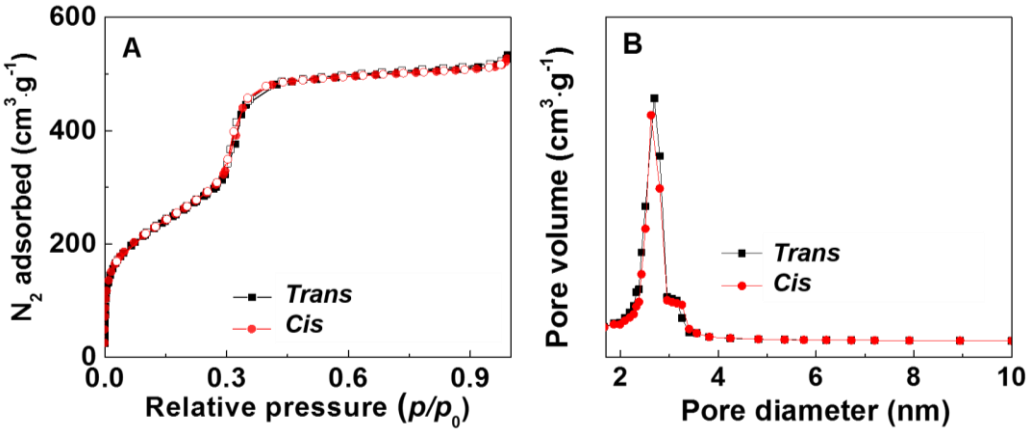

Figure S10. (A) N_2 adsorption-desorption isotherms and (B) pore size distributions of the sample AM-3 of *trans* and *cis* configuration.

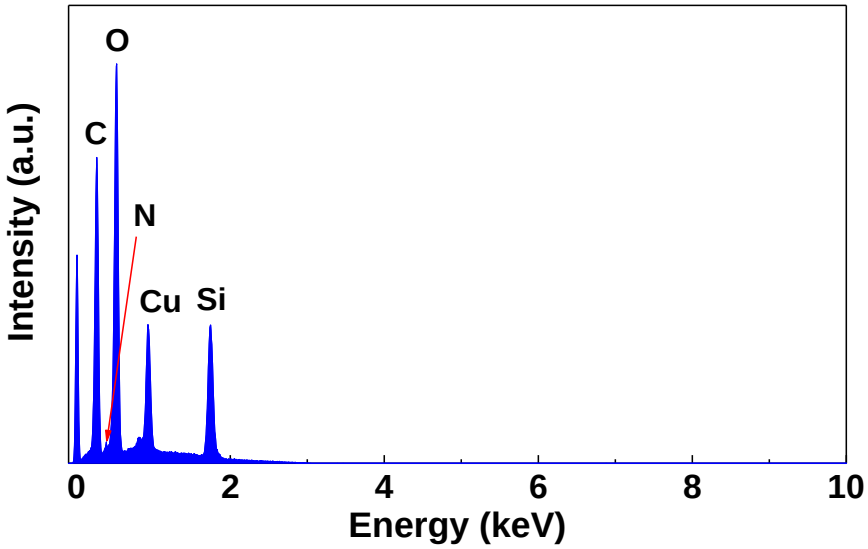

Figure S11. Energy dispersive X-ray spectroscopy of the sample AM-3. The element Cu is originated from the Cu grid used in the measurement.

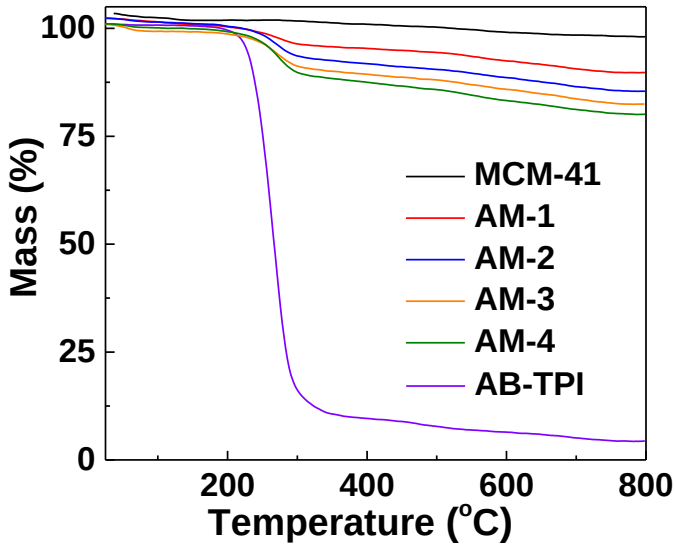

Figure S12. TG curves of AB-TPI, MCM-41, and AB-modified MCM-41 samples.

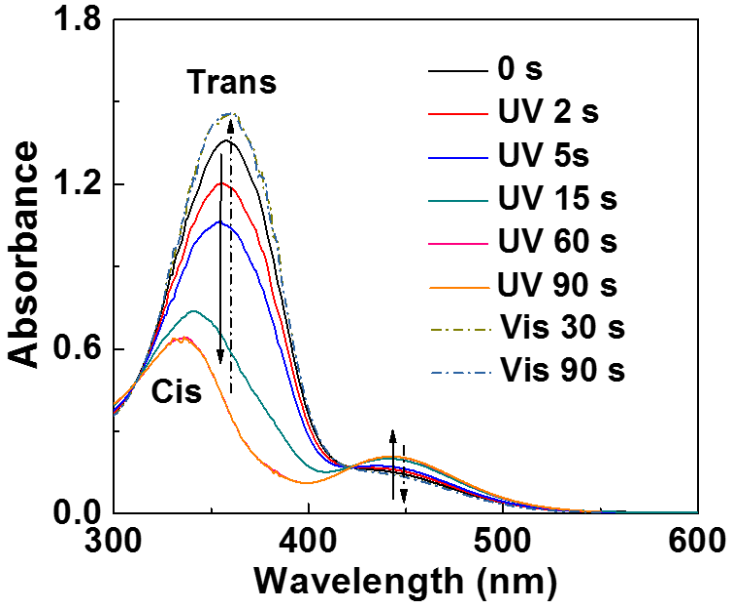

Figure S13. Changes in the UV-vis spectra of AB-TPI isomerization, following different UV/Visible light irradiation time.

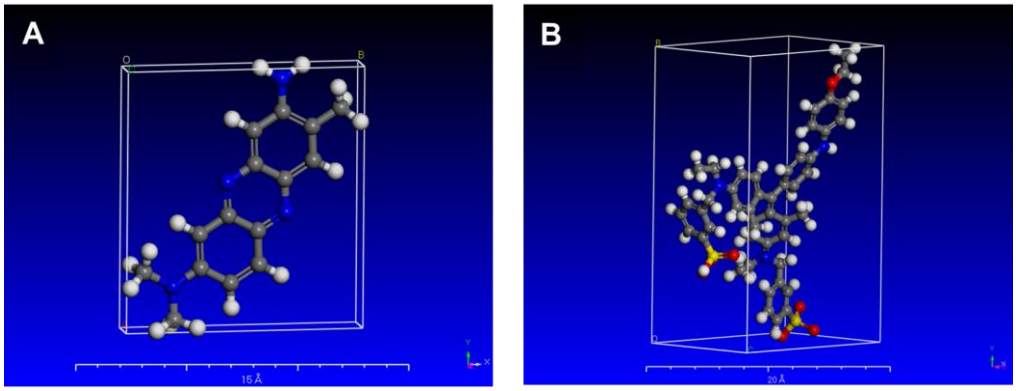

Figure S14. The molecular structure of dye molecules (A) neutral red (NR) and (B) Coomassie brilliant blue (CBB).

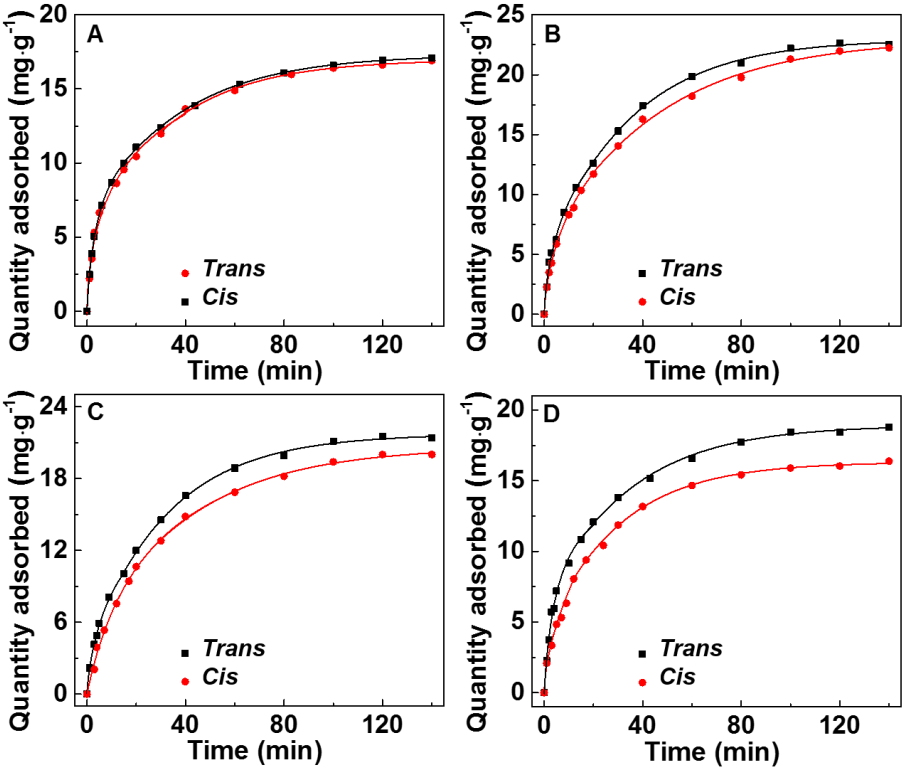

Figure S15. Adsorption dynamic curves of NR on the adsorbent (A) MCM-41, (B) AM-1, (C) AM-2, and (D) AM-4 of *trans* and *cis* configuration.

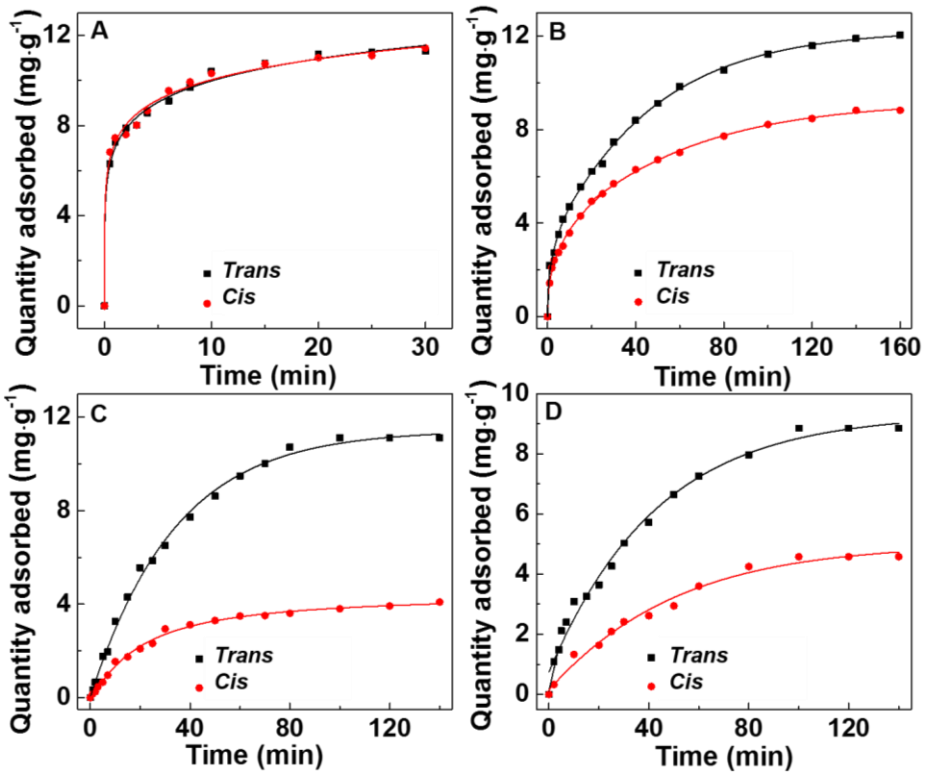

Figure S16. Adsorption dynamic curves of CBB on the adsorbent (A) MCM-41, (B) AM-1, (C) AM-2, and (D) AM-4 of *trans* and *cis* configuration.